

Semimonthly oscillation observed in the start time of equatorial plasma bubbles

Spread-F

Igo Paulino¹, Ana Roberta Paulino², Ricardo Yvan de la Cruz Cueva³, Ebenezer Agyei-Yeboah⁴, Ricardo Arlen Buriti¹, Hisao Takahashi⁵, Cristiano Max Wrasse⁵, [Angela M. Santos](#)⁵, Amauri Fragoso de Medeiros¹, and [Inez S. Batista](#)⁵

¹Unidade Acadêmica de Física, Universidade Federal de Campina Grande, Campina Grande, Brazil

²Departamento de Física, Universidade Estadual da Paraíba, Campina Grande, Brazil

³Departamento de Física, Universidade Estadual do Maranhão, São Luís, Brazil

⁴Instituto de Pesquisa e Desenvolvimento, Universidade do Vale do Paraíba, São José dos Campos, Brazil

⁵Divisão de Aeronomia, Instituto Nacional de Pesquisas Espaciais, São José dos Campos, Brazil

Correspondence: Igo Paulino (igo.paulino@df.ufcg.edu.br)

Abstract.

Using [airglow](#) data from ~~airglow the~~ an all sky imager ~~and a coherent backscatter radar~~ deployed at São João do Cariri (7.4°S, 36.5°W) ~~and São Luís (2.6°S, 44.2°W), respectively~~, the start time of equatorial [equatorial plasma bubbles](#) Spread-F were studied ~~in order to investigate the day-to-day variability of this phenomenon~~. Data from a period ~~of~~ over 10 years was ~~analysed~~ ~~investigated~~ from 2000 to 2010. ~~The~~ Semimonthly oscillations were clearly revealed in the start time of plasma bubbles from OI6300 airglow images during ~~this period of observation~~ and ~~four case studies~~ (September 2003, September-October 2005, November 2005 and January 2008) ~~were chosen to show in details this kind of modulation~~. Since the airglow measurements are not continuous in time, more than one cycle of oscillation in the start time of plasma bubbles cannot be observed from these data. Thus, ~~data from a digisonde of São Luís (2.6°S, 44.2°W) in November 2005 were used to corroborate the result~~ ~~of coherent backscatter radar data appeared as an alternative to investigate the start time of the ionospheric irregularities~~. Semimonthly ~~oscillation were observed in the start time of plumes (November 2005) and bottom type Spread-F (November 2008) with at least one complete cycle~~. Technical/climate issues did not ~~allow~~ ~~allowed~~ to observe the semimonthly oscillations simultaneously by the two instruments, but from ~~October to November~~ ~~September to December~~ 2005 there was a predominance of this ~~spread-F start-time~~ oscillation in the start time of the irregularities over Brazil. Besides, statistical analysis for the data in whole period ~~of observation has shown that the lunar tide, which has semimonthly variability, must be the main forcing for the semimonthly oscillation in the start time of equatorial plasma bubbles~~. The presence of this oscillation certainly contribute to the day-to-day variability of [equatorial plasma bubbles](#) spread-F.

Keywords: Spread-F, Plasma bubble, Semimonthly oscillation, [Lunar tide](#), [16d planetary wave](#) [Plumes](#).

1 Introduction

Equatorial plasma bubbles (EPBs) appear in the bottom side of the F-region in the equatorial ionosphere when there is an unstable F-layer. It generally occurs after the pre-reversal enhancement (PRE), after sunset. The pre-reversal enhancement

consists of a rapid up shift of the F layer before the motion of the plasma be downward reverted. The main mechanism used to explain the development of the EPBs is the Rayleigh-Taylor (RT) instability. According to ~~this~~ theory, the RT growth rate is inversely proportional to the collision frequency between the neutral and ionic particles and it is proportional to the plasma density gradient. Thus, when the PRE is strong, it becomes more probable for EPBs occur.

5 In addition, the RT instability process needs a seeding mechanism, which has been largely studied in the last decades. Some researchers have pointed out gravity waves as seeding to the EPB (e.g., Fritts et al., 2008; Abdu et al., 2009; Takahashi et al., 2009; Taori et al., 2011; Paulino et al., 2011). Other studies have marked the dynamics of post sunset vortex and PRE dynamics as enough to the EPB origin (e.g., Kudeki and Bhattacharyya, 1999; Kudeki et al., 2007; Eccles et al., 2015; Tsunoda et al., 2018; Huang, 2018). The thermospheric neutral wind system and the associated electrodynamics have also been proposed as
10 sufficient to the EPB appearance as well (e.g., Saito and Maruyama, 2009). Influences of magnetic storms and large scale waves have also been reported as important mechanism to the day-to-day variability of EPBs (e.g., Abalde et al., 2009; Huang et al., 2013).

Actually, observations have shown that there is a strong day-to-day variability of the EPB occurrence and development (e.g., Carter et al., 2014; Abdu, 2019) and it is a topic of current research. There is evidence of planetary waves acting in the neutral
15 winds and consequently changing the background condition of the atmosphere (e.g., Forbes, 1996; Takahashi et al., 2006; Abdu and Brum, 2009; Chang et al., 2010; Zhu et al., 2017).

Stening and Fejer (2001) published the first work proposing the influence of lunar tides in the probability of occurrence of EPBs. It is well ~~known~~ that the main component of the lunar tides has a semimonthly ~~oscillation~~
20 ~~oscillations~~. Based on these factors, the present work shows, ~~for the first time~~, that there are semimonthly oscillations ~~statistically significant~~ in the ~~start time of EPBs observed by airglow images throughout the period of observations.~~
~~EPB, Plumes and Bottom Type Spread-F start time in different epochs of observations.~~ Besides, these oscillations follow the Moon phases. These results can indicate strong evidences of the lunar semidiurnal tide modulating the wind system in the F region and consequently it is driving the time of generation of Spread-F.

2 Data Analysis

25 Airglow measurements of the OI 630.0 nm (OI6300) have been recorded at São João do Cariri (7.4°S, 36.5°W) since September 2000. In this investigation, data from September 2000 to December 2010 were used, which corresponds to the first generation of the all sky imager deployed in this observatory.

The all sky imager is composed by a fish eye lens, a telecentric set of lens, a filter wheel, a set of lens to reconstruct the image, a Charge Coupled Device (CCD) chip and a cooling system. This instrument has a field of view of 180° of the sky.
30 Further details of this imager have been published elsewhere (e.g., Paulino et al., 2016). Airglow images of the OI6300 were taken by about 15 days around the New Moon with integration time of 90 s. Depending on the mode of operation, images can have 2-4 min of temporal resolution. The start and end times can be extracted directly from the image header after observing the appearance or disappearance of the structures. The start time was defined as the time when the plasma bubbles appeared in

the images. It generally occurs in the Northwest part of the images. After that, the plasma bubbles start their development and dynamics.

Figure 1 shows an example of the determination of the start time of EPBs on 27 January 2001. The supplementary short movie can help one to identify the time, in which the plasma bubbles start to extend to the southern part of the images.

- 5 Corroborative data from a Digisonde Portable Sounder (DPS) installed at São Luís (2.6°S, 44.2°W) were also used to identify the time of maximum vertical drift of the F layer, which corresponds to the time of the pre-reversal enhancement. This instrument consist in variable high frequency radar. In order to calculate the vertical plasma drifts were estimated from ionograms, which are charts of the frequency versus virtual height. The DPS system has taken ionograms every 10 min. Data collected in October 2003, October 2005 and November 2005 were investigated. However, semimonthly oscillation in the time
- 10 of maximum vertical drift of the F layer were observed only in November 2005 and it will be discussed in ahead. Further details about the digisonde deployed at São Luís and the methodology of determination of the vertical plasma drifts from ionograms have been published elsewhere (e.g., Resende et al., 2019).
- 15 ~~coherent VHF backscatter radar deployed at São Luís (2.6°S, 44.2°W) were also used to identify the start time of plume and bottom type spread F (BTSF) structures. The data ranged from 02 September 2001 to 31 December 2008. The VHF coherent radar of São Luís operates at 30 MHz with a power peak of 4 kW. It has antenna half-power full-beam-width of 10° and inter-pulse-period of 9.34 ms. The coverage in altitude of 87.5 to 1267 km and velocity of $\pm 250 \text{ ms}^{-1}$. The altitude resolution is 2.5 km and noise band-width of 120 kHz. These characteristics allow to observe irregularities of 5 m in the ionosphere. Further technical details of the São Luís' radar can be found in de Paula and Hysell (2004) and Rodrigues et al. (2008).~~

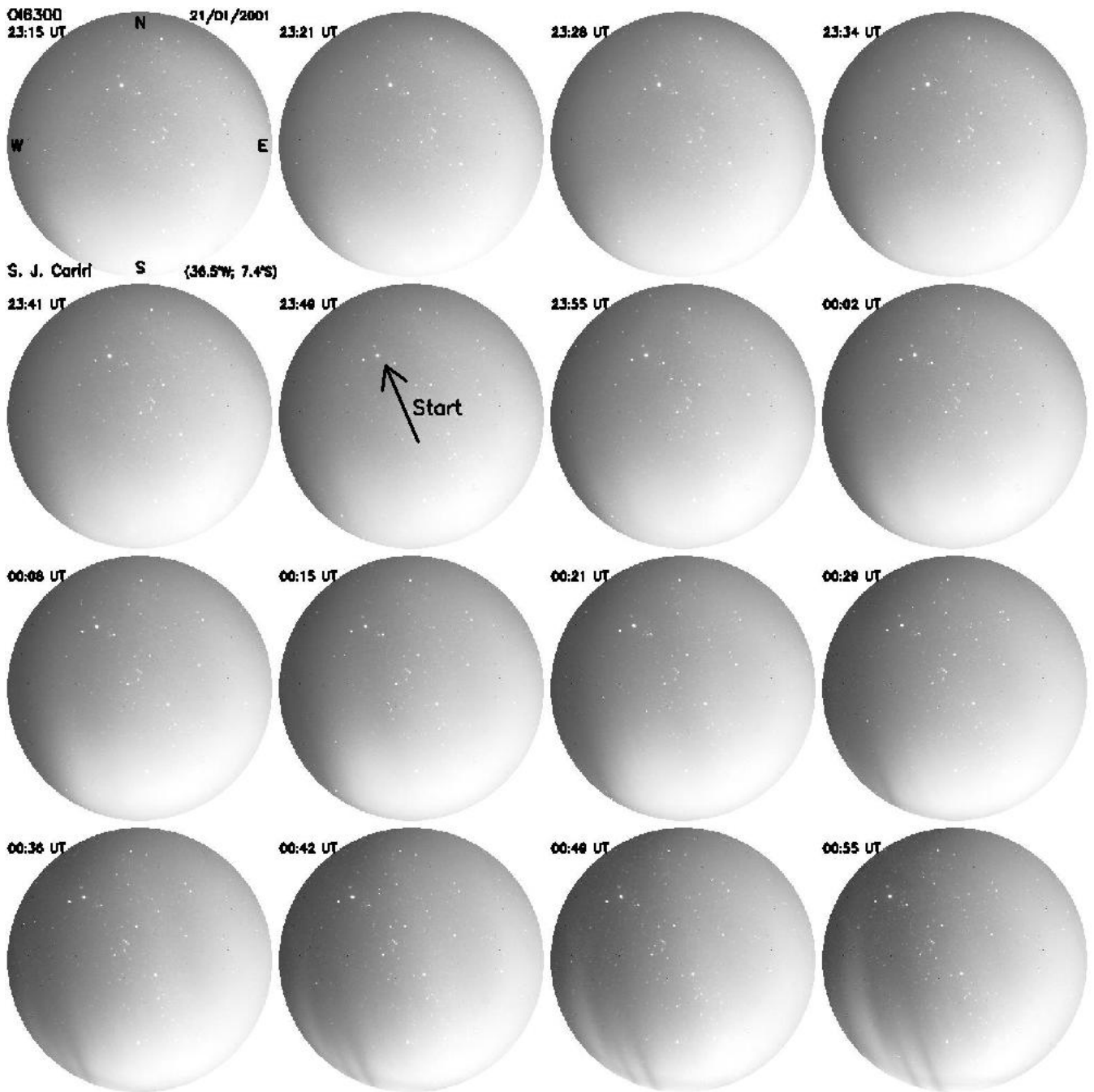


Figure 1. Sequence of OI6300 airglow images observed in São João do Cariri on 27 January 2001. One can observe the start time of the EPB on this night.

~~Start time of Plume and BTSF were defined in Cueva et al. (2013). Those parameters correspond to the exact time of appearance of plumes and BTSFs in the range time integration (RTI) maps. The temporal resolution of the start time of the spread-F calculated in the RTI maps were 12 min.~~

3 Results and Discussion

5 Figure 2(a) shows the evolution of ~~the~~ start time of the EPBs observed in September 2003 over São João do Cariri. The solid line represents the best fit for a periodicity of 14.5 days, the stars correspond to the exact time in which the plasma bubble appeared in the OI6300 images and the filled circle shows the New Moon time. In this case, one can see a good ~~agreement~~ of the fit line with the observation during a half cycle of the oscillation. The amplitude of this oscillation was calculated from the fitting as ~ 52 min, i.e., there was a difference of ~ 52 min in the start time of EPBs along the observed nights.

10 Figure 2(b) shows the best fit 14.5 days oscillation in the start time of EPBs observed from the later September to early October 2005. For the whole period of airglow observation, it was the best case study observed because it covers a full circle of the oscillation. There was an amplitude of ~ 37 min and the position of the New Moon was observed on 03 October ~~2005~~²⁰⁰⁵. The predominance of this oscillation ~~in the start time of EPBs~~ persists up to November 2005 as shown in Figure 2(c) with higher amplitude ~ 70 min.

15 Similar results to September 2003 and November 2005 were found in January 2008 as one can see in Figure 2(d), inclusive the position of the New Moon in the cycle. The estimated amplitude was ~ 45 min.

The results from Figure 2 indicate that the start time of EPBs was modulated by a semimonthly oscillation. Besides, the results shown here, in other period of observation there were observed a tendency of the start time following this periodicities. However, only few days, less than a half month, were observed and those results are not shown here. ~~Additionally, long term~~
20 ~~statistical analysis will be discussed in ahead~~.

The present work concentrate the discussion on the cases in which, a half cycle could be observed. Semimonthly oscillations well known in the atmosphere are: (1) Quasi 16 days planetary waves and (2) Lunar semidiurnal tide.

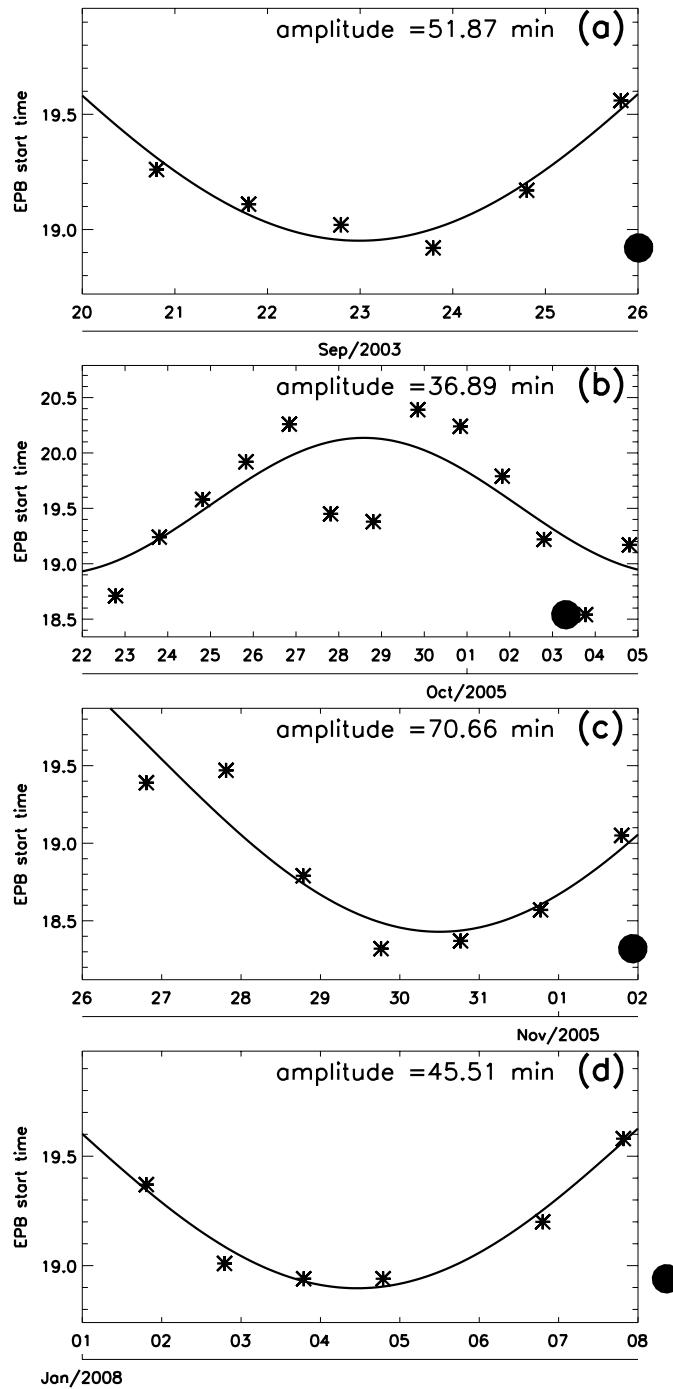


Figure 2. Start time of plasma bubble (stars) as function of time. Solid line represents the best fit to a sinusoidal oscillation with period of 14.5 days. The respective amplitudes are shown on the middle top of the panels. Panel (a) shows the results for September 2003. Panel (b) shows the results for September - October 2005. Panel (c) shows the results for October-November 2005. Panel (d) shows the results for January 2008. Filled circles indicate the New Moons.

Simulations have shown that the 16d planetary waves (PWs) have large amplitudes in the winter hemisphere at the lower levels of the atmosphere and high latitudes, but above the mesosphere, there is a penetration of this wave to the summer hemisphere, which allows that it can be observed in both hemispheres including in the equatorial region (Miyoshi, 1999).

Forbes and Leveroni (1992) have pointed out that 16d oscillation in the E and F-region could be connected by the upward propagation of Rossby wave from the winter stratosphere. Although, the 16d PW has a well defined seasonality in the lower atmosphere, according to the simulations, in the upper atmosphere the presence of this oscillation has been predicted to be more spread along the year (Miyoshi, 1999). It is also important to mention that the 16d oscillations were observed in the mesosphere and lower thermosphere from 85 to 100 km altitude in the equatorial region in the zonal wind during the period around the September equinox and solstices of 1994 (Luo et al., 2002), which coincides to the periods of observation of the results of Figure 2 present results.

Lunar semidiurnal tides have been pointed out as important factor to the appearance and the start time of EPBs (e.g., Stening and Fejer, 2001). The main reason for the influence of the lunar tides in the EPB variability is the capability of the lunar tides propagate upward to high levels of the atmosphere and consequently it can affect the pre-reversal enhancement (PRE) amplitude and time (Stening and Fejer, 2001). Another factor to be considered is the moon phase (New Moon) that coincides to zero position of the oscillation for all observed cases, including the case studied observed from the DPS coherent backscatter radar that will be shown ahead. The real mechanism that allows the lunar tides to act in the PRE is not well defined, but some works have pointed out as either the direct propagation to the bottom side of ionospheric F region (e.g., Evans, 1978; Forbes, 1982) or coupling of the E region dynamo to the F region (e.g., Immel et al., 2009; Eccles et al., 2011).

In order to corroborate the present results, data from the DPS backscatter radar deployed in São Luís have been used to investigate the time of maximum vertical drifts, which is directly associated to the PRE. start time of the bottom type spread-F (BTSE) and plumes. The main goal of these analysis is trying to observe more this kind of oscillation in other ionospheric parameter. Although the DPS operates continuously every day, i.e., the digisonde does not depend on the tropospheric weather conditions, only a half cycle of the oscillation could be observed in the used data. than one cycle of the semimonthly oscillation in the start time of spread-F, since the radar was operating continuously and does not depend on tropospheric weather conditions.

Figure 3 shows the temporal evolution of the time of the maximum vertical drift observed from the DPS data in early November 2005. An amplitude of $\sim 46min$ was calculated, indicating that the PRE is sensible to the semimonthly oscillation as well. An important factor to these observations was that this oscillation acted in the ionosphere for a long period, since the start time of EPBs from later September (Figure 2b). There were simultaneous measurements of the start time of EPBs and the time of maximum vertical drifts in October 2005. However, the latter have not present reliable results for the semimonthly oscillation. a complete cycle of 14.5 days in the start time of plume observed on November 2005, which coincide with the same period of observation of EPBs in the airglow images. For this case, an amplitude of ~ 1 hour was observed.

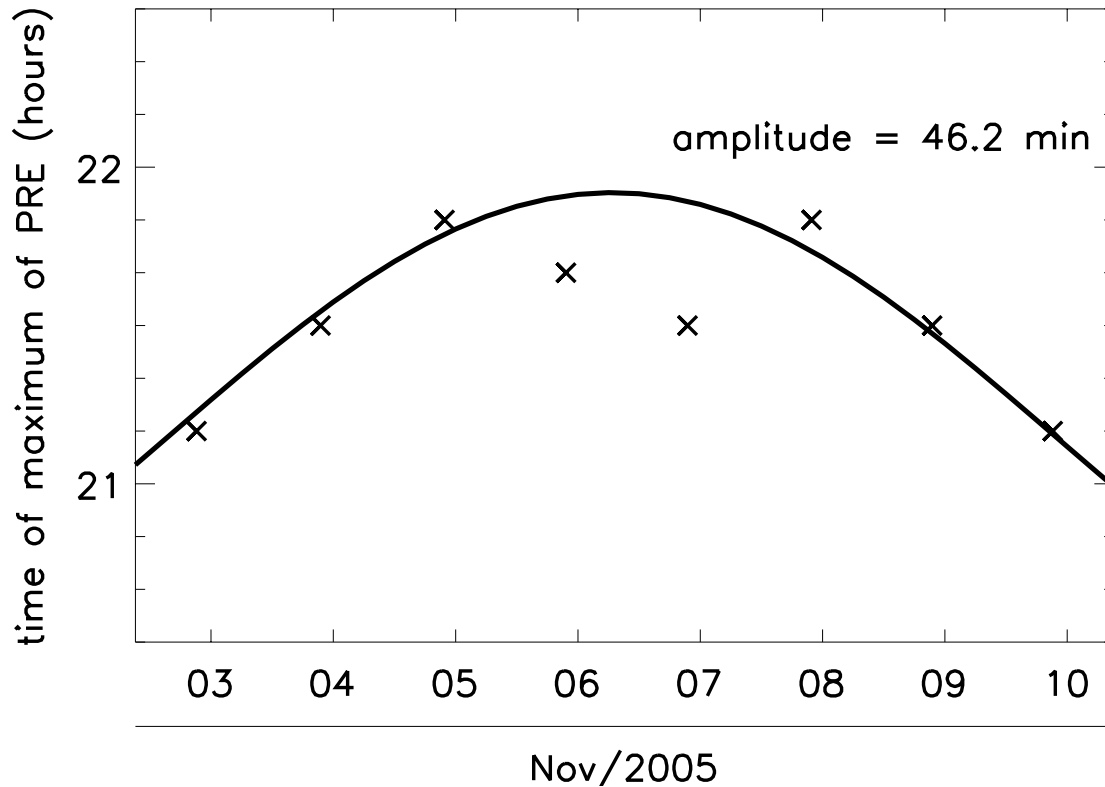


Figure 3. Same as Figure 2, but for time of maximum of vertical drift of the F layer. ~~start time of plumes. Open circles indicate the Full Moon.~~

Figures 2 and 3 ~~Figures 3 and 4~~ show that the ionospheric parameters ~~spread-F structures~~ can be controlled by the semimonthly oscillation ~~oscillation~~. However, the strong day-to-day variability of the spread-F does not allow to observe this signature always. Another difficulty in the ~~DPS radar~~ data analysis was the algorithm does not give an exact start time of the oscillation, i.e., there was a temporal resolution of ~~10-15~~ min in this determination.

- 5 Although as the performed fit to the start time of EPBs as the fitting to the time of maximum vertical drifts of the F layer presented high amplitudes and very good agreements to the observation, only one case studied presented an almost full cycle (Figure 2b). Then, a statistical analysis was done in order to observe the relevance of this approach and how much frequent is the modulation of the semimonthly oscillation in the start time of EPBs. This analysis was performed considering the potential effect of the lunar tides in the ionosphere as simulated and discussed by (Stening and Fejer, 2001). In order to do that, a
- 10 methodology described by (?) has also been used.

Figure 4 shows solar local time of the start time of EPBs as a function of the local lunar time for all period of observation of the all sky airglow camera. Note that only the start time of EPBs around of the sunset was considered, i.e., plasma bubbles that appeared in the airglow mages no later than 21:10 solar local time. ~~the start time evolution of the bottom type spread-F in~~

November 2008, one can observe two complete cycles of the start time of the BTSF fitting a semi-month oscillation with an amplitude of ~ 12 min.

The lunar time was calculated as $\tau = t - \nu$, where, t is the local solar time and ν is the age of the Moon, which depends on the phases of the Moon. Further details about the calculation of the lunar time can be found in Paulino et al. (2017) and references therein. In Figure 4, solid line represents the best fit for a 12 hours oscillation, which released an amplitude of ~ 11 min and standard deviation of the fitted curve is shown by the dashed lines.

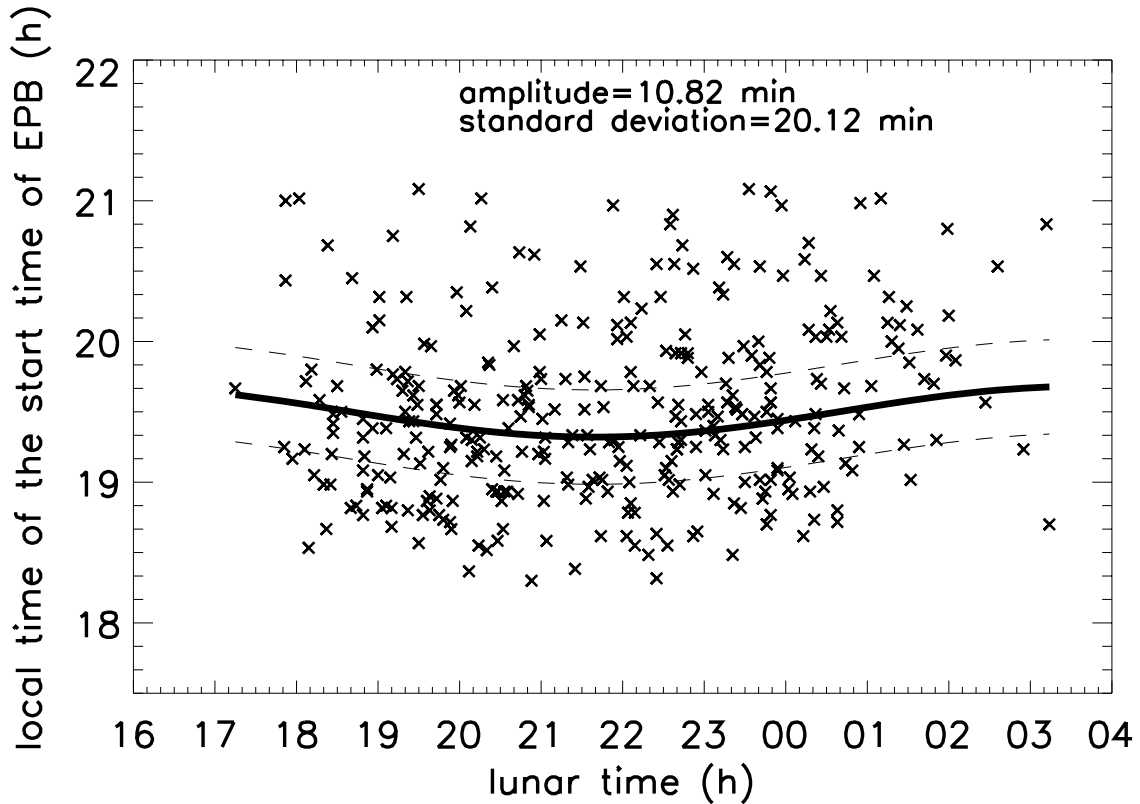


Figure 4. Start time of the EPBs (local time) as function of the lunar local time for whole period of observations. Same as Figure 3, but for start time of bottom-type spread-F.

From the results of Figure 4, it is clear that the semimonthly oscillation is always present the start time of EPBs with a significant amplitude. These results are statistically significant and it was released that this kind of semimonthly oscillation is always present in the start time of EPBs. It suggests that the lunar semidiurnal tide, which has a well defined semimonthly variation, has an important role in the time of occurrence of EPBs. Previous studies have pointed out the lunar semidiurnal tide can modulated ionospheric parameters such as the height and critical frequency of the F layer, PRE drifts, etc. The present

results strongly suggest that the generation of EPBs are affected as well. Further analysis of the start time of Spread-F, using radar measurements will be important in the advances of the knowledge of the day-to-day variability of EPBs.

4 Summary

Using almost one solar cycle of data from OI630 airglow images ~~and range-time integration maps from a backscatter radar in the equatorial region over Brazil~~, semimonthly oscillations in the start time of ~~EPBs~~ spread-F (EPBs, BTSF and Plumes) were observed and the results are summarized as follow:

- Four periods of airglow observation showed amplitudes higher than 36 min in the start time of EPBs for 14.5 days oscillation, three periods of observations (September 2003, October 2005 and January 2008) revealed good fit for half cycle and the another case (September 2005) showed and complete cycle;
- 10 – DPS measurements from São Luís showed semimonthly oscillation in the maximum vertical drifts of the F region related to the PRE ~~Two complete cycles of 14.5 days with amplitude of ~ 12 min were observed in the bottom type spread-F in November 2008;~~
- Statistical analysis in the whole period of observations of EPBs in the airglow images revealed semimonthly oscillations are always present in the start time of EPBs, when the lunar time was considered. Thus, it strongly suggest that the lunar semidiurnal tide has an important role the start time of EPBs. ~~Plumes observed in the RTI data showed a 14.5 cycle oscillation with amplitude of 1 hour in the start time of plumes during November 2005;~~
- 15

The present results indicate that one semimonthly dynamical structure can control either the start time or the amplitude of the PRE that can consequently produce ~~EPBs~~ Spread-F. These results must contribute to understanding the day-to-day variability of equatorial ~~plasma bubbles~~ spread-F. However, the results ~~shows~~ that besides the semimonthly oscillations, other phenomena are important to the day-to-day variability occurrence of EPBs since this oscillations is not dominant in the whole period of observation. Regarding to the agents that are causing this oscillation, further investigation are necessary, however, semidiurnal lunar tides appeared as an important phenomenon to the time of the appearance of EPBs. ~~and they are out of the scope of this work. Lunar semidiurnal tides, which have semimonthly period of oscillation have been pointed out as a likely agent to produce this kind of oscillation in the start time of Spread-F. Besides, we have discussed the importance of 16d PWs that must be further investigated before being neglected.~~

20

25

Data availability. All sky image data can be requested from either the Aerolume (UFCEG) or Lume (INPE) Groups to the e-mail address to the first author of the manuscript. DPS ionograms can be requested to Dr. Inez S. Batista (inez.batista@inpe.br) ~~RTI maps can be requested from the Dr. Ricardo Y. C. Cueva (navivaeu@gmail.com);~~

Author contributions. IP has written the manuscript and made most of the airglow analysis. ARP has discussed the semimonthly oscillation due to lunar tides and 16d planetary waves. RYCC has contributed to the discussion on the start time of EPBs ~~calculated the start time of bottom type spread F and plumes and provide technical information about the coherent radar~~. EA-Y has reduced the whole image data calculating the start time of EPBs. RAB has contributed to run the experiments in São João do Cariri and help with the analysis. HT has contributed to the discussion of 16d oscillation. AMS has evaluated the time of maximum vertical drifts of the F layer. AFM has provide some computing codes to work with the OI6300 airglow images. ISB has provided the DPS data for analysis.

Competing interests. The authors declare that they do not have competing interests;

Acknowledgements. I. Paulino thanks to Conselho Nacional de Desenvolvimento Científico e Tecnológico (CNPq) for the financial support (303511/2017-6). A. R. Paulino thanks to the Coordenação de Aperfeiçoamento de Pessoal de Nível Superior (CAPES) for the scholarship and CNPq by the grant (# 460624/2014-8).

References

- Abalde, J. R., Sahai, Y., Fagundes, P. R., Becker-Guedes, F., Bittencourt, J. A., Pillat, V. G., Lima, W. L. C., Candido, C. M. N., and de Freitas, T. F.: Day-to-day variability in the development of plasma bubbles associated with geomagnetic disturbances, *Journal of Geophysical Research: Space Physics*, 114, <https://doi.org/10.1029/2008JA013788>, 2009.
- 5 Abdu, M. A.: Day-to-day and short-term variabilities in the equatorial plasma bubble/spread F irregularity seeding and development, *Progress in Earth and Planetary Science*, 6, 11, <https://doi.org/10.1186/s40645-019-0258-1>, 2019.
- Abdu, M. A. and Brum, C. G. M.: Electrodynamics of the vertical coupling processes in the atmosphere-ionosphere system of the low latitude region, *Earth, Planets and Space*, 61, 385–395, <https://doi.org/10.1186/BF03353156>, 2009.
- Abdu, M. A., Alam Kherani, E., Batista, I. S., de Paula, E. R., Fritts, D. C., and Sobral, J. H. A.: Gravity wave initiation of equatorial
10 spread F/plasma bubble irregularities based on observational data from the SpreadFEx campaign, *Annales Geophysicae*, 27, 2607–2622, <https://doi.org/10.5194/angeo-27-2607-2009>, 2009.
- Carter, B. A., Yizengaw, E., Retterer, J. M., Francis, M., Terkildsen, M., Marshall, R., Norman, R., and Zhang, K.: An analysis of the quiet time day-to-day variability in the formation of postsunset equatorial plasma bubbles in the Southeast Asian region, *Journal of Geophysical Research: Space Physics*, 119, 3206–3223, <https://doi.org/10.1002/2013JA019570>, 2014.
- 15 Chang, L. C., Palo, S. E., Liu, H.-L., Fang, T.-W., and Lin, C. S.: Response of the thermosphere and ionosphere to an ultra fast Kelvin wave, *Journal of Geophysical Research: Space Physics*, 115, <https://doi.org/10.1029/2010JA015453>, 2010.
- Cueva, R. Y. C., de Paula, E. R., and Kherani, A. E.: Statistical analysis of radar observed F region irregularities from three longitudinal sectors, *Annales Geophysicae*, 31, 2137–2146, <https://doi.org/10.5194/angeo-31-2137-2013>, 2013.
- de Paula, E. R. and Hysell, D. L.: The São Luís 30 MHz coherent scatter ionospheric radar: System description and initial results, *Radio
20 Science*, 39, <https://doi.org/10.1029/2003RS002914>, 2004.
- Eccles, J. V., St. Maurice, J. P., and Schunk, R. W.: Mechanisms underlying the prereversal enhancement of the vertical plasma drift in the low-latitude ionosphere, *Journal of Geophysical Research: Space Physics*, 120, 4950–4970, <https://doi.org/10.1002/2014JA020664>, 2015.
- Eccles, V., Rice, D. D., Sojka, J. J., Valladares, C. E., Bullett, T., and Chau, J. L.: Lunar atmospheric tidal effects in the
25 plasma drifts observed by the Low-Latitude Ionospheric Sensor Network, *Journal of Geophysical Research: Space Physics*, 116, <https://doi.org/10.1029/2010JA016282>, 2011.
- Evans, J. V.: A note on lunar tides in the ionosphere, *Journal of Geophysical Research: Space Physics*, 83, 1647–1652, <https://doi.org/10.1029/JA083iA04p01647>, 1978.
- Forbes, J. M.: Atmospheric tide: 2. The solar and lunar semidiurnal components, *Journal of Geophysical Research: Space Physics*, 87, 5241–5252, <https://doi.org/10.1029/JA087iA07p05241>, 1982.
- 30 Forbes, J. M.: Planetary Waves in the Thermosphere-Ionosphere System, *Journal of geomagnetism and geoelectricity*, 48, 91–98, <https://doi.org/10.5636/jgg.48.91>, 1996.
- Forbes, J. M. and Leveroni, S.: Quasi 16-day oscillation in the ionosphere, *Geophysical Research Letters*, 19, 981–984, <https://doi.org/10.1029/92GL00399>, 1992.
- Fritts, D. C., Vadas, S. L., Rigglin, D. M., Abdu, M. A., Batista, I. S., Takahashi, H., Medeiros, A., Kamalabadi, F., Liu, H.-L., Fejer, B. G., and
35 Taylor, M. J.: Gravity wave and tidal influences on equatorial spread F based on observations during the Spread F Experiment (SpreadFEx), *Annales Geophysicae*, 26, 3235–3252, <https://doi.org/10.5194/angeo-26-3235-2008>, <https://www.ann-geophys.net/26/3235/2008/>, 2008.

- Huang, C.-S.: Effects of the postsunset vertical plasma drift on the generation of equatorial spread F, *Progress in Earth and Planetary Science*, 5, 3, <https://doi.org/10.1186/s40645-017-0155-4>, 2018.
- Huang, C.-S., de La Beaujardière, O., Roddy, P. A., Hunton, D. E., Ballenthin, J. O., Hairston, M. R., and Pfaff, R. F.: Large-scale quasiperiodic plasma bubbles: C/NOFS observations and causal mechanism, *Journal of Geophysical Research: Space Physics*, 118, 3602–3612, <https://doi.org/10.1002/jgra.50338>, 2013.
- Immel, T. J., England, S. L., Zhang, X., Forbes, J. M., and DeMajistre, R.: Upward propagating tidal effects across the E- and F-regions of the ionosphere, *Earth, Planets and Space*, 61, 505–512, <https://doi.org/10.1186/BF03353167>, 2009.
- Kudeki, E. and Bhattacharyya, S.: Postsunset vortex in equatorial F-region plasma drifts and implications for bottomside spread-F, *Journal of Geophysical Research: Space Physics*, 104, 28 163–28 170, <https://doi.org/10.1029/1998JA900111>, 1999.
- 10 Kudeki, E., Akgiray, A., Milla, M., Chau, J. L., and Hysell, D. L.: Equatorial spread-F initiation: Post-sunset vortex, thermospheric winds, gravity waves, *Journal of Atmospheric and Solar-Terrestrial Physics*, 69, 2416 – 2427, <https://doi.org/https://doi.org/10.1016/j.jastp.2007.04.012>, vertical Coupling in the Atmosphere/Ionosphere System, 2007.
- Luo, Y., Manson, A. H., Meek, C. E., Meyer, C. K., Burrage, M. D., Fritts, D. C., Hall, C. M., Hocking, W. K., MacDougall, J., Riggan, D. M., and Vincent, R. A.: The 16-day planetary waves: multi-MF radar observations from the arctic to equator and comparisons with the HRDI measurements and the GSWM modelling results, *Annales Geophysicae*, 20, 691–709, <https://doi.org/10.5194/angeo-20-691-2002>, <https://www.ann-geophys.net/20/691/2002/>, 2002.
- 15 Miyoshi, Y.: Numerical simulation of the 5-day and 16-day waves in the mesopause region, *Earth, Planets and Space*, 51, 763–772, <https://doi.org/10.1186/BF03353235>, 1999.
- Paulino, A. R., Lima, L. M., Almeida, S. L., Batista, P. P., Batista, I. S., Paulino, I., Takahashi, H., and Wrasse, C. M.: Lunar tides in total electron content over Brazil, *Journal of Geophysical Research: Space Physics*, 122, 7519–7529, <https://doi.org/10.1002/2017JA024052>, 2017.
- 20 Paulino, I., Takahashi, H., Medeiros, A., Wrasse, C., Buriti, R., Sobral, J., and Gobbi, D.: Mesospheric gravity waves and ionospheric plasma bubbles observed during the COPEX campaign, *Journal of Atmospheric and Solar-Terrestrial Physics*, 73, 1575 – 1580, <https://doi.org/https://doi.org/10.1016/j.jastp.2010.12.004>, influence of Solar Activity on Interplanetary and Geophysical Phenomena, 2011.
- 25 Paulino, I., Medeiros, A. F., Vadas, S. L., Wrasse, C. M., Takahashi, H., Buriti, R. A., Leite, D., Filgueira, S., Bageston, J. V., Sobral, J. H. A., and Gobbi, D.: Periodic waves in the lower thermosphere observed by OI630 nm airglow images, *Annales Geophysicae*, 34, 293–301, <https://doi.org/10.5194/angeo-34-293-2016>, 2016.
- Resende, L. C. A., Denardini, C. M., Picanço, G. A. S., Moro, J., Barros, D., Figueiredo, C. A. O. B., and Silva, R. P.: On developing a new ionospheric plasma index for the Brazilian equatorial F region irregularities, *Annales Geophysicae Discussions*, 2019, 1–20, <https://doi.org/10.5194/angeo-2019-42>, <https://www.ann-geophys-discuss.net/angeo-2019-42/>, 2019.
- 30 Rodrigues, F. S., Hysell, D. L., and de Paula, E. R.: Coherent backscatter radar imaging in Brazil: large-scale waves in the bottomside F-region at the onset of equatorial spread F, *Annales Geophysicae*, 26, 3355–3364, <https://doi.org/10.5194/angeo-26-3355-2008>, 2008.
- Saito, S. and Maruyama, T.: Effects of transequatorial thermospheric wind on plasma bubble occurrences, *Journal of the National Institute of Information and Communications Technology*, 56, 257–266, 2009.
- 35 Stening, R. J. and Fejer, B. G.: Lunar tide in the equatorial F region vertical ion drift velocity, *Journal of Geophysical Research: Space Physics*, 106, 221–226, <https://doi.org/10.1029/2000JA000175>, 2001.

Takahashi, H., Wrasse, C. M., Pancheva, D., Abdu, M. A., Batista, I. S., Lima, L. M., Batista, P. P., Clemesha, B. R., and Shiokawa, K.: Signatures of 3-6 day planetary waves in the equatorial mesosphere and ionosphere, *Annales Geophysicae*, 24, 3343–3350, <https://doi.org/10.5194/angeo-24-3343-2006>, 2006.

5 Takahashi, H., Taylor, M. J., Pautet, P.-D., Medeiros, A. F., Gobbi, D., Wrasse, C. M., Fechine, J., Abdu, M. A., Batista, I. S., Paula, E., Sobral, J. H. A., Arruda, D., Vadas, S. L., Sabbas, F. S., and Fritts, D. C.: Simultaneous observation of ionospheric plasma bubbles and mesospheric gravity waves during the SpreadFEx Campaign, *Annales Geophysicae*, 27, 1477–1487, <https://doi.org/10.5194/angeo-27-1477-2009>, <https://www.ann-geophys.net/27/1477/2009/>, 2009.

10 Taori, A., Patra, A. K., and Joshi, L. M.: Gravity wave seeding of equatorial plasma bubbles: An investigation with simultaneous F region, E region, and middle atmospheric measurements, *Journal of Geophysical Research: Space Physics*, 116, <https://doi.org/10.1029/2010JA016229>, 2011.

Tsunoda, R. T., Saito, S., and Nguyen, T. T.: Post-sunset rise of equatorial F layer—or upwelling growth?, *Progress in Earth and Planetary Science*, 5, 22, <https://doi.org/10.1186/s40645-018-0179-4>, 2018.

Zhu, Z., Luo, W., Lan, J., and Chang, S.: Features of 3–7-day planetary-wave-type oscillations in F-layer vertical drift and equatorial spread F observed over two low latitude stations in China, *Annales Geophysicae*, 35, 763–776, <https://doi.org/10.5194/angeo-35-763-2017>, 2017.

15 List of changes

	Replaced: plasma bubbles	1
	Added: Angela	1
	Added: M. Santos	1
	Added: Inez	1
20	Added: S. Batista	1
	Added: airglow	1
	Deleted: airglow the	1
	Deleted: and a coherent backscatter radar	1
	Deleted: and São Luís (2.6°S, 44.2°W), res ...	1
25	Replaced: equatorial plasma bubbles	1
	Added: in order to investigate the day-to- ...	1
	Deleted: of	1
	Replaced: analysed	1
	Deleted: The	1
30	Replaced: this period of observation	1
	Added: four case studies	1
	Added: were chosen to show in details this ...	1
	Replaced: data from a digisonde of São Luís ...	1
	Deleted: Semimonthly oscillation were obs ...	1

	Replaced: allow	1
	Replaced: October to November	1
	Deleted: spread-F start time	1
	Added: in the start time of the irregularities	1
5	Added: Besides, statistical analysis for the ...	1
	Replaced: equatorial plasma bubble	1
	Replaced: Lunar tide, 16d planetary wave	1
	Replaced: this	2
	Replaced: known	2
10	Replaced: oscillation	2
	Added: for the first time,	2
	Added: statistically significant	2
	Replaced: start time of EPBs observed by air ...	2
	Added: ,	2
15	Replaced: Digisonde Portable Sounder (DPS ...	3
	Deleted: Start time of Plume and BTSF we ...	5
	Deleted: Those parameters correspond to th ...	5
	Added: the	5
	Replaced: agreement	5
20	Replaced: 2005	5
	Added: in the start time of EPBs	5
	Added: ,	5
	Added: Additionally, long term statistical ...	5
	Added: ,	7
25	Added: that	7
	Replaced: can	7
	Replaced: has	7
	Replaced: results of Figure 2	7
	Added: (e.g., Stening and Fejer, 2001)	7
30	Replaced: study	7
	Replaced: DPS	7
	Replaced: DPS	7
	Replaced: time of maximum vertical drifts, w ...	7
	Replaced: this kind of oscillation in other ion ...	7
35	Replaced: the temporal evolution of the time ...	7

	Replaced: time of maximum of vertical drift...	8
	Replaced: Figures 2 and 3	8
	Replaced: ionospheric parameter	8
	Deleted: the	8
5	Replaced: oscillations	8
	Replaced: DPS	8
	Replaced: 10	8
	Added: Although as the performed fit to t...	8
	Replaced: solar local time of the start time of...	9
10	Added: The lunar time was calculated as ...	9
	Replaced: Start time of the EPBs (local time)...	9
	Added: From the results of Figure 4, it is ...	10
	Deleted: and range time integration maps fr...	10
	Replaced: ‘	10
15	Replaced: DPS measurements from São Luís...	10
	Replaced: Statistical analysis in the whole pe...	10
	Replaced: EPBs	10
	Replaced: plasma bubbles	10
	Replaced: show	10
20	Replaced: however, semidiurnal lunar tides a...	10
	Replaced: DPS ionograms can be requested ...	10
	Replaced: contributed to the discussion on th...	11
	Added: AMS has evaluated the time of ma ...	11
	Added: ISB has provided the DPS data for ...	11